

supplementary material and method

1 **METHOD AND MATERIAL**

2 **Dataset's analysis**

3 The CRC-related RNA-sequencing dataset GSE84984 was obtained from the Gene Expression
4 Omnibus (GEO) database. The GSE84984 dataset contains nine tumor tissues and six normal tissues.
5 Then, we filtered the background noise of the gene expression profile and then performed the data
6 analysis using R software. Next, the differentially expressed lncRNAs were identified as follows:
7 FDR (adjusted p-value) <0.05 and $|\log_2\text{-fold change}|>1$. Differential expression analysis was
8 performed using the “limma” package in R. In addition, a volcano plot was generated to show the
9 upregulated and downregulated lncRNAs. The top10 downregulated and upregulated lncRNAs are
10 shown in the heatmap.

11 To analyze the expression of SNHG16 and the prognosis of CRC patients, we performed overall
12 survival analysis. First, TCGA-COAD RNA-seq was obtained from TCGA website, including 480
13 tumor tissues and 41 normal tissues (<https://portal.gdc.cancer.gov/>). Then, duplicated data or patients
14 without survival information were excluded. Finally, a total of 467 samples enrolled in our survival
15 analysis research.

16 **Patient samples**

17 The Research Ethics Committee approved this study of Wuhan University (Wuhan, Hubei, PR China).
18 Informed consent was obtained from all participating patients. The enrolled patients were diagnosed
19 with primary CRC by histopathologic diagnosis, underwent surgeries and had complete prognostic
20 information. No patients received local or systemic neoadjuvant radiotherapy or/and chemotherapy
21 and targeted therapy. One hundred and eleven human CRC tissues and PANTs (distance to cancer $>$
22 5 cm) were randomly obtained from patients in the Zhongnan Hospital of Wuhan University between
23 January 2014 and December 2015. Each sample was snap-frozen in liquid nitrogen and then stored
24 at -80°C .

25 **Cell culture and treatment**

26 The human colon cancer cell lines DLD1, Caco2, SW480, SW620, HT29, Iovo, and HCT116 and the
27 normal intestinal epithelium cell line NCM460 were obtained from the Cell Bank of Wuhan
28 University. Cells were maintained in an incubator at 37°C and 5% CO_2 . Cells were cultured in DMEM
29 (Gibco, USA) supplemented with 2 mmol/L glutamine and 10% fetal calf serum (Gibco, USA).

supplementary material and method

30 **Plasmid construction, siRNAs, miRNA, transfections, and infection.**

31 miR-195-5p mimics and inhibitor (Table S2) were obtained from RiboBio Co. Ltd., China. The
32 SNHG16 expression lentiviral vector (NR_038108.1), YAP1 expression lentiviral vector
33 (NM_001130145), and TEAD1 lentiviral expression vector (NM_021961) were chemically
34 synthesized, constructed, sequenced and identified by Shanghai GeneChem Chemical Technology,
35 Co. Ltd. (Shanghai, China). The SNHG16 overexpression lentiviral vector (NR_038108.1) was
36 chemically synthesized, constructed, sequenced and identified by Wuhan GeneCopoeia Technology,
37 Co. Ltd. (Wuhan, China). The siRNA, shRNA, lentiviral vector of SNHG16, YAP1, and TEAD1
38 were chemically synthesized, constructed, sequenced and identified by Shanghai Genepharma
39 Technology, Co. Ltd. The sequence of corresponding shRNA for plasmid construction was placed in
40 supplementary table 1. For transfection, siRNA and plasmid were transfected into CRC cells using
41 Lipofectamine 2000 transfection reagent (Invitrogen, Carlsbad, CA). For infection, we performed
42 according to the manufacturer's instructions. First, we obtained the multiplicity of infection (MOI)
43 values of HCT116 (MOI = 10) and DLD1 (MOI = 20) cells. For virus infection, virus and polybrene
44 (final 7 µg/ml, Sigma Aldrich, Cat# 107689) were added to cells with 25% confluence. Fresh media
45 was added 16 h after infection. The medium was changed to medium containing appropriate
46 antibiotics 48 h after infection. After puromycin selection, the cells were maintained for at least one
47 day without drug for further experiments.

48 **qRT-PCR and subcellular fractionation**

49 Total RNA was extracted from tissue samples and cell lines using the TRIzol Reagent (Invitrogen,
50 USA) according to the manufacturer's instructions. A Nanodrop2000 was used to quantify RNA
51 concentration, and 1µg of total RNA was reverse transcribed into cDNA. We performed cDNA
52 synthesis from mRNA by using the Primescript™ RT Reagent Kit (Vazyme, Nanjing, China; R223-
53 01). cDNA synthesis for microRNA detection was carried out using miRNA 1st Strand cDNA
54 Synthesis Kit (Vazyme, Nanjing, China; MR101-01/02). cDNA of microRNA was used for
55 subsequent qRT-PCR using SYBR-Green PCR Master Mix (Vazyme, Nanjing, China; MQ101-
56 01/02). cDNA of mRNA and lncRNA was used for subsequent qRT-PCR using SYBR-Green PCR
57 Master Mix (Vazyme, Nanjing, China; Q311-02/03). The amplification conditions for cDNA of
58 mRNA were as follows: 95°C for 2min, followed by 40 circles of 95°C for 5s, 60°C for 30s, and 72 °C
59 for 30s. Each reaction was run on a BioRad IQ5 Real-time PCR instrument (BioRad, USA). Relative
60 expression was calculated using the $2^{-\Delta\Delta Ct}$ method. The primer sequences are listed in Table S1
61 (Supplementary Table 1).

supplementary material and method

62 According to the manufacturer's instructions, cytosolic and nuclear fractions of HCT116 and DLD1
63 were isolated by the Nuclear/Cytoplasmic Extraction Kit (Cayman, USA). Subsequently, the RNA
64 levels of a nuclear control transcript (U6), cytoplasmic control transcript (GAPDH), and SNHG16
65 were analyzed by qRT-PCR.

66 **Protein extraction, western blotting, and protein quantification**

67 Cells were lysed using RIPA buffer supplemented with complete proteinase inhibitor cocktail
68 (Thermo Scientific, USA, Cat.No.89900). The detail of lyse process was introduced in the
69 introduction of RIPA. Put it simply, we used 400ul of buffer per 25 cm² flask (or 150ul per well in
70 six-well plate). Then, the lysate was homogenized using sonication, and the impurities were removed
71 by high-speed centrifugation (13000rpm × 20min). Finally, the total proteins were quantified using
72 the BCA reaction. Total proteins were separated by SDS-PAGE and subsequently transferred to
73 PVDF membranes (Millipore, USA). Prior to incubation with diluted primary antibodies and HRP-
74 conjugated secondary antibodies, blots were blocked in nonfat milk for an hour. The primary
75 antibodies and dilution ratios were as follows: anti-E-cadherin (1:1000; CST, USA), anti-Vimentin
76 (1:1000; Proteintech, China), anti-YAP1 (1:1000; Proteintech, China), and anti-GAPDH (1:5000;
77 CST, USA). Quantitation of protein on all WB has been performed by Image J, and the results were
78 normalized by the blank group. Finally, all the bar graphs of protein quantitation were placed on a
79 supplementary file.

80 **Luciferase reporter assay**

81 For miR-195-5p target assay, the luciferase vector of YAP1 were chemically synthesized, constructed,
82 sequenced and identified by RiboBio Technology, Co. Ltd. (Guangzhou, China)¹. Likewise,
83 SNHG16 fragments containing the putative binding sites for miR-195-5p were also synthesized,
84 constructed, sequenced and identified by RiboBio Technology, Co. Ltd. (Guangzhou, China). Put it
85 simply, the 3'-UTR sequences of YAP1 (WT and mut) and miR-195-5p binding sites in SNHG16
86 (WT and mut) were amplified from genomic DNA (human source). Then, the purified products of
87 PCR products were connected to the pmiR-RB-Report plasmid (Promega, USA), which has similar
88 cleavage sites of restriction enzyme with PCR products (5': XhoI; 3': NotI), with DNA ligase.
89 Following transformation of *Escherichia coli* with recombinant plasmid DNA, the positive bacterial
90 colony was screened by Ampicillin. The sequence and primers used in this process had been placed
91 in supplementary table 1. For the SNHG16 promoter assay, the SNHG16 promoter (-2000/+1) and

supplementary material and method

92 modified constructs (-1861/+1, -1794/+1, -1368/+1) were amplified from the genomic DNA (human
93 source) and inserted into the pGL3-Basic plasmid (Promega, USA). Then, the cDNA of the SNHG16
94 promoter containing the predicted TEAD1 binding sites was subcloned into the pGL3-Basic vector
95 (Promega, USA), termed PGL3-SNHG16-pro (RiboBio Co. Ltd., China). Then, the TEAD1 binding
96 site mutated SNHG16 promoter was synthesized by RiboBio (RiboBio Co. Ltd., China), termed as
97 pGL3-SNHG16-pro-mut (1 and 2). According to the manufacturer's instructions, the transfection was
98 carried out using Lipofectamine 2000, and luciferase activities were determined using the dual-
99 Luciferase reporter system (Promega, USA).

100 **Colony formation, CCK8, and wound healing assay**

101 For colony formation detection, HCT116 cells were placed in 6-well plates at a density of 1000 cells
102 per well. In the same way, DLD1 cells were placed at a density of 1000 cells per well. After two
103 weeks of culture in an incubator, the cells were fixed with 4% paraformaldehyde and stained with
104 0.5% crystal violet. To perform a CCK8 assay, we seeded the cells in 96-well plates with the cell
105 density of 3.0×10^3 cells/well in 100 μ L DMEM. After incubating for 0h, 24h, 48h, 72h, 96h, each well
106 was put in 10 μ L CCK8 (Biosharp, China) and incubated for 2h at 37°C. Finally, the OD values of
107 cells was measured at a wavelength of 450 nm by Multiskan FC microplate absorbance reader
108 (Thermo Fisher, USA). A wound healing assay was also used to measure the migratory capacity of
109 CRC cells. Cells were seeded in 6-well plates and allowed to grow until the confluence reached 90%.
110 A 20 μ l pipette tip was used to scrap several lines across the cell surface, and then plates were washed
111 three times to remove nonadherent debris. Finally, the cells were incubated at 37°C with a serum-free
112 medium, and photos were taken every 12 hours. The data analysis and process of wound healing are
113 similar as Simona Martinotti ²

114 **Transwell migration and invasion assay**

115 Twenty-four-well Transwell (8 μ m pore size; Corning, USA) were used to assess the cell migration
116 and invasion ability of CRC cells. For migration assay, 1.0×10^5 cells in 0.4 ml serum-free DMEM
117 medium were seeded on the upper surface of the well. For the invasion assay, Transwell chambers
118 were coated with Matrigel, and 1.5×10^5 cells were seeded on the upper surface of the chamber in 0.4
119 ml serum-free medium. After 36 - 48 h of incubation, cells on the upper surface of the chamber were
120 removed with cotton swabs, and the remaining cells on the lower surface of the chamber were fixed
121 and stained with 0.5% crystal violet solution.

122 **Xenograft assays**

supplementary material and method

123 The animal experiment was approved by the ethical committee of Zhongnan Hospital of Wuhan
124 University and performed in accordance with the Guide for the Care and Use of Laboratory Animals
125 of Wuhan University. To perform the tumor proliferation assay, 12 BALB/c nude mice (4-6 weeks
126 old) (Hubei Research Center of Laboratory Animals, China) were randomly divided into three groups
127 (n = 4 per group): HCT116/ Lv-anti-SNHG16 NC, HCT116/ Lv-anti-SNHG16 + Lv-Oe-YAP1 NC,
128 and HCT116/ Lv-anti-SNHG16 + Lv-Oe-YAP1. In total, 5×10^6 HCT116 cells suspended in 200 μ l
129 medium were subcutaneously injected into the right flank of mice. After ten days, subcutaneous tumor
130 size was measured by digital Vernier calipers every 1 week, and the subcutaneous tumor volume was
131 calculated by the following formula: volume = $1/2 \times (\text{length} \times \text{width}^2)$. After thirty days, the
132 transplantable tumor and 1ml mouse blood were collected for further research. For the metastasis
133 experiment, the mice were randomly divided into three groups (n = 6 per group). The stable cell line
134 was injected into the mice via the tail vein, and metastasis was assessed 30 days after injection by
135 dissection. Finally, the mice were euthanized and necropsied to assess metastatic burden. Then, we
136 further examined the tumor tissues, liver and lung tissues by hematoxylin and eosin (H&E) staining,
137 Immunohistochemistry (IHC) staining and RT-PCR assay. Protein quantification in IHC was also
138 represented by integral optic density (IOD), which is normalized by negative control group.

139 **Statistical analysis**

140 All the data were derived from at least three independent experiments, and p values < 0.05 were
141 considered statistically significant. Through SPSS statistical software and GraphPad Prism software,
142 all statistical analyses were performed. To assess the association between SNHG16 expression and
143 YAP1, and miR-195-5p expression, we used Pearson's correlation analysis. Then, we applied the chi-
144 square test to analyze the expression of SNHG16 and the clinicopathological status of CRC patients.
145 Means of continuous outcome variables were appropriately tested with one-way analyses of variance or two-
146 tailed Student's t-test. Groups of discrete variables were compared by means of the Mann-Whitney *U* test or
147 Kruskal-Wallis nonparametric analysis of variance. In addition, Kaplan-Meier survival curves and log-
148 rank tests were used for survival analysis. Finally, univariate and multivariate Cox-regression
149 analyses were applied to identify the independent factors of prognosis.

150

supplementary tables

Supplementary Table 1: The sequences of the primers and shRNA

Gene	Primer Sequence (5' – 3')	
SNHG16	F: AGCAGAATGCCATGGTTTCC	R: GGTCAATTTAGGGCACGGTCT
TWIST1	F: CACTGAAAGGAAAGGCATCA	R: GGCCAGTTTGATCCCAGTAT
HMGA2	F: ACCCAGGGGAAGACCCAAA	R: CCTCTTGCCGTTTTTCTCCA
FoxQ1	F: CACGCAGCAAGCCATATACG	R: CGTTGAGCGAAAGGTTGTGG
Snail2	F: CGAACTGGACACACATACAGTG	R: CTGAGGATCTCTGGTTGTGGT
Snail1	F: TCGGAAGCCTAACTACAGCGA	R: AGATGAGCATTGGCAGCGAG
PRX1	F: CCCGATGCTTTTGTTCGAGA	R: CATGTGGCAGAATAAGTAGCCAT
ZEB2	F: AGGAGCAGGTAATCG	R: TGGGCACTCGTAAGG
ZEB1	F: CGAGTCAGATGCAGAAAATGAGCAA	R: ACCCAGACTGCGTCACATGTCTT
YAP1	F: CTTCTCCCGGGATGTCTCAG	R: TCAAGGTAGTCTGGGAAACGG
miR -195 -5p RT	CTCAACTGGTGTCGTGGAGTCGGCAATTCAGTTGAGGCCAATAT	
miR -195 -5p	F: CGCAGCACAGAAATATTGGC	R: CTCAACTGGTGTCGTGGAGTC
U6 RT	R: AACGCTTCACGAATTTGCGT	
U6	F: CTCGCTTCGGCAGCACA	R: AACGCTTCACGAATTTGCGT
TEAD1	F: TGCGCAAAGAAGAATGGTAGA	R: TGCGCAAAGAAGAATGGTAGA
ChIP primer site1	F: GAAAGGAACTATGTTTGCAGGGA	R: CATTGAGCAGTAATTCTGGCCA
ChIP primer site2	F: AGGAGAATCACTTGAGCTTGGG	R: GAAAGGAACTATGTTTGCAGGGA
TEAD1_s hRNA	5'-CACCGCTTGAATCAGTGGACATTCGCGAACGAATGTCCACTGATTCAAGC -3'	
SNHG16_s hRNA	5'-AATTCAAAAAAGCCTCTGCTGCTAATTGTTCTCTTGAACAATTAGCAGCAGAGGCG -3'	
YAP1_s hRNA	5'-CACCGCTTGAATCAGTGGACATTCGCGAACGAATGTCCACTGATTCAAGC -3''	
h-YAP1-3'UTR-WT	F: GCGCTCGAGTGCAGTTTTTCAGGCTAATACAGA	R: AATGCGGCCCGCAGGATACATTCCACTACCACACTA
h-YAP1-3'UTR-MUT	F: CCTTGTCATACGACGAGTTAATGTATTGCTGACCTCTT	R: ATACATTAACCTCGTCGTATGGACAAGGAAGACAAAATA
h-SNHG16 -3UTR WT	F: GCGCTCGAGTAGCTCCAGCGATGCCAGA	R: AATGCGGCCCGCCACTGATATTCTATGCAAAGATCTG
h-SNHG16 -3UTR MUT	F: CTGCTCACGACGAAATTGTTCTCTAAAGTAATCG	R: GAACAATTTGCTCGTGAGGCAGGGCTGTGCTGA

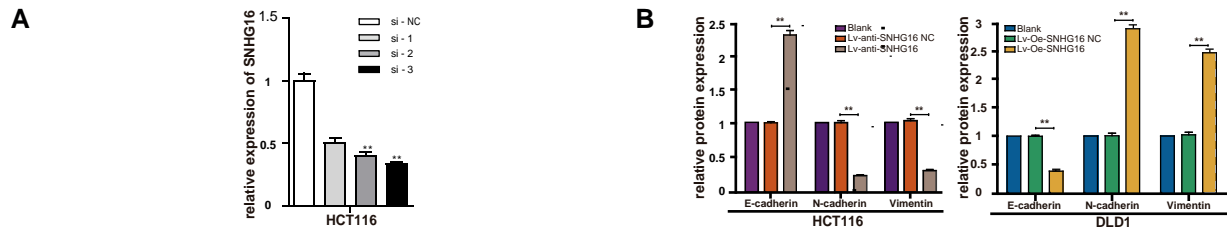
supplementary tables

Supplementary Table 2: The sequence of miR-195-5p inhibitor and mimics

Gene	Primer Sequence (5' – 3')
Mimics	Sense : UAGCAGCACAGAAAUAUUGGC Antisense : GCCAAUAUUUCUGUGCUGCUA
Mimics NC	Sense: UUUGUACUACACAAAAGUACUG Antisense: CAGUACUUUUGUGUAGUACAAA
Inhibitor	GCCAAUAUUUCUGUGCUGCUA
Inhibitor NC	CAGUACUUUUGUGUAGUACAAA

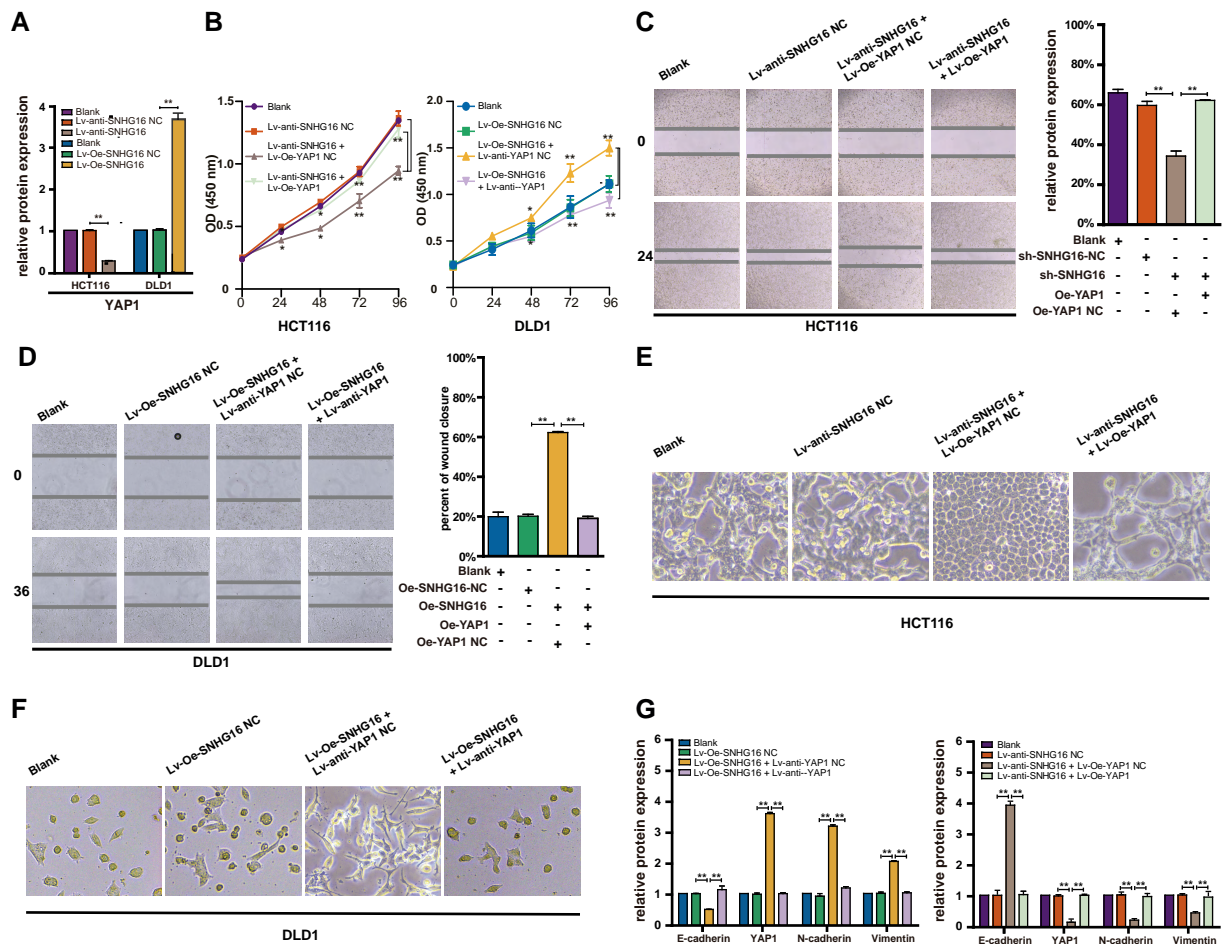
supplementary figures

Supplementary Fig 1. The ectopic expression of SNHG16 affects proliferation and EMT of CRC cells



A: The knockdown effect of SNHG16 siRNA was validated by qRT-PCR. **B:** The protein quantitation of EMT markers expression from SNHG16 overexpression or knockdown CRC cell lines were shown as bar graphs. Statistical analysis was conducted using one-way ANOVA. $**p < 0.01$; Error bars, SEM.

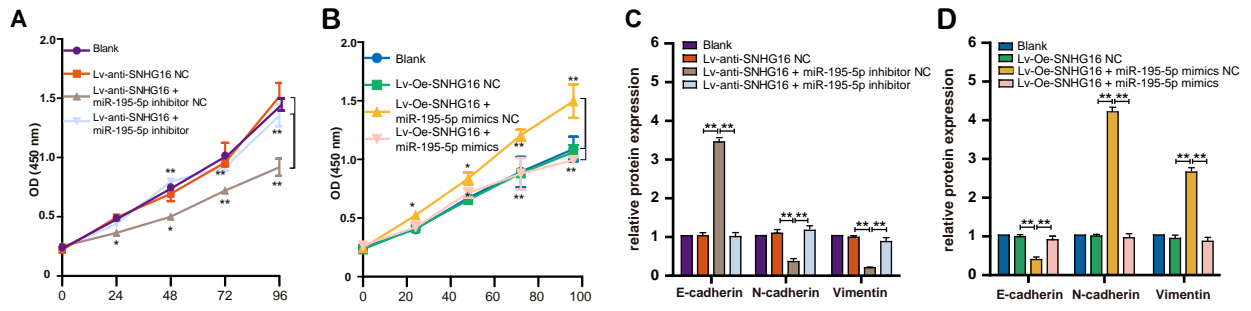
Supplementary Fig 2. SNHG16 facilitates CRC cellular proliferation, migration, and EMT in a YAP1-dependent manner.



A: The protein quantitation of YAP1 expression from SNHG16 overexpression or knockdown CRC cell lines were shown as bar graphs. **B:** CCK8 cell proliferation assay in HCT116 (HCT116^{Blank}, HCT116^{Lv-anti-SNHG16-NC}, HCT116^{Lv-anti-SNHG16 + Lv-Oe-YAP1-NC}, and HCT116^{Lv-anti-SNHG16 + Lv-Oe-YAP1}) and DLD1 (DLD1^{Blank}, DLD1^{Lv-Oe-SNHG16 NC}, DLD1^{Lv-Oe-SNHG16 + Lv-anti-YAP1-NC}, DLD1^{Lv-Oe-SNHG16 + Lv-anti-YAP1}). **C:** The migration in HCT116^{Blank}, HCT116^{Lv-anti-SNHG16-NC}, HCT116^{Lv-anti-SNHG16 + Lv-Oe-YAP1-NC}, and HCT116^{Lv-anti-SNHG16 + Lv-Oe-YAP1} was detected by wound healing assay. **D:** The migration in DLD1^{Blank}, DLD1^{Lv-Oe-SNHG16 NC}, DLD1^{Lv-Oe-SNHG16 + Lv-anti-YAP1-NC}, and DLD1^{Lv-Oe-SNHG16 + Lv-anti-YAP1} was detected by wound healing assay. All representative data are from three independent experiments. **E:** Photomicrographs of HCT116^{Blank}, HCT116^{Lv-anti-SNHG16-NC}, HCT116^{Lv-anti-SNHG16 + Lv-Oe-YAP1-NC}, and HCT116^{Lv-anti-SNHG16 + Lv-Oe-YAP1}. **F:** Photomicrographs of DLD1^{Blank}, DLD1^{Lv-Oe-SNHG16 NC}, DLD1^{Lv-Oe-SNHG16 + Lv-anti-YAP1-NC}, DLD1^{Lv-Oe-SNHG16 + Lv-anti-YAP1}. **G:** The protein quantitation of YAP1 and EMT markers expression from eight different cell lines were shown as bar graphs. Statistical analysis was conducted using one-way ANOVA. Error bars, SEM. $**p < 0.01$.

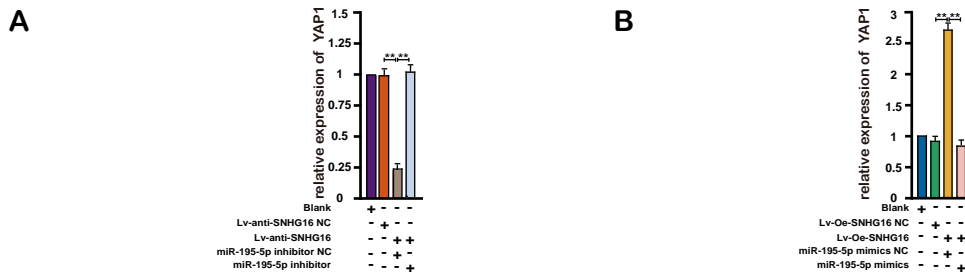
supplementary figures

Supplementary Fig 3. miR-195-5p could potentially abrogate the effect of SNHG16/YAP1 axis on tumor progression.



A-B: CCK8 cell proliferation assay in HCT116 (A) and DLD1 (B). **C:** The protein quantitation of EMT markers expression from HCT116^{Blank}, HCT116^{Lv-anti-SNHG16-NC}, HCT116^{Lv-anti-SNHG16 + miR-195-5p inhibitor NC} and HCT116^{Lv-anti-SNHG16 + miR-195-5p inhibitor} were shown as bar graphs. **D:** The protein quantitation of EMT markers expression from DLD1^{Blank}, DLD1^{Lv-Oe-SNHG16-NC}, DLD1^{Lv-Oe-SNHG16 + miR-195-5p mimics NC}, and DLD1^{Lv-Oe-SNHG16 + miR-195-5p mimics} were shown as bar graphs. Statistical analysis was conducted using one-way ANOVA. Error bars, SEM. ***p* < 0.01

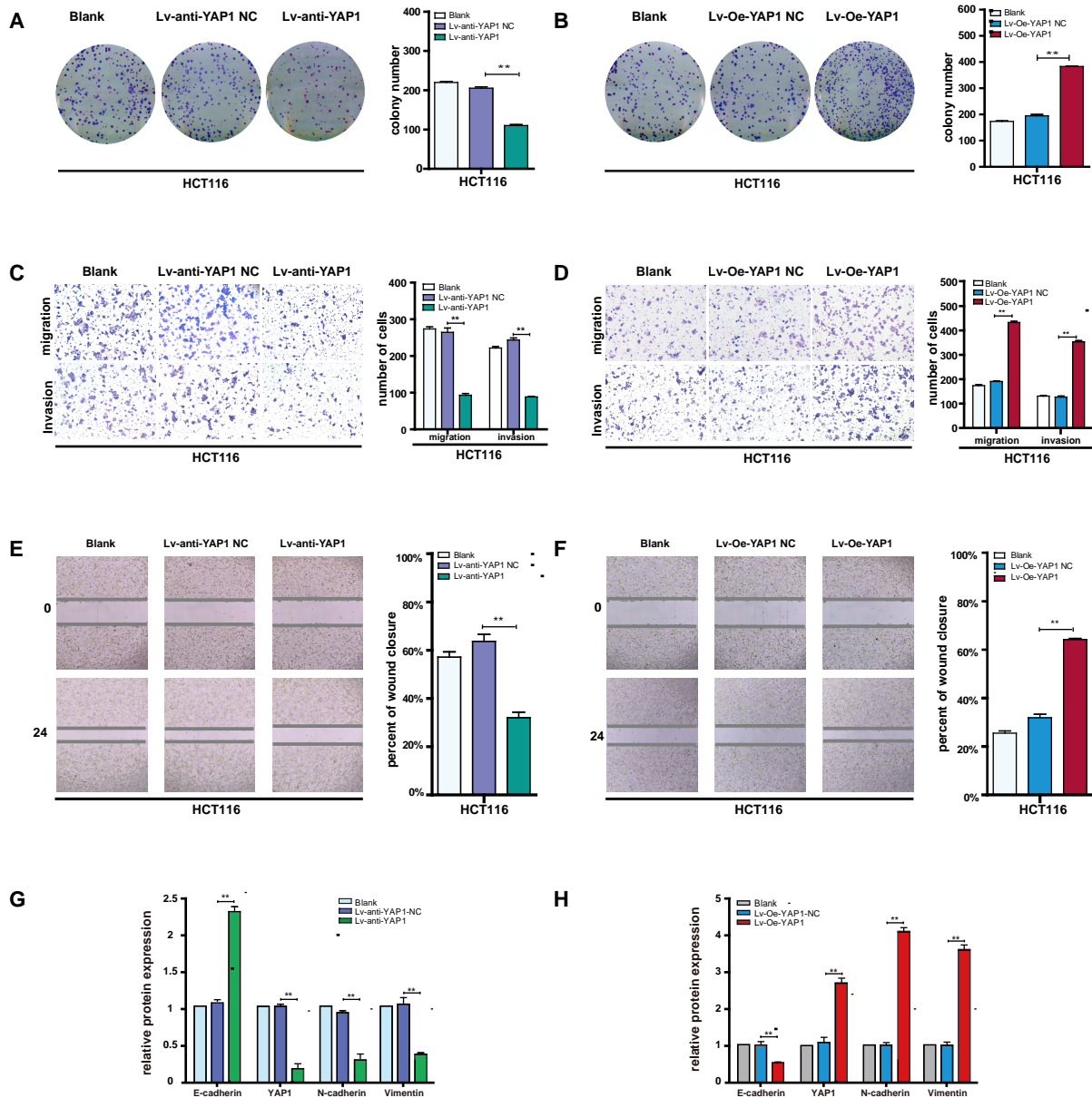
Supplementary Fig 4. SNHG16 functions as a ceRNA and sponges miR-195-5p, further regulating YAP1 expression.



A: The protein quantitation of YAP1 expression from HCT116^{Blank}, HCT116^{Lv-anti-SNHG16-NC}, HCT116^{Lv-anti-SNHG16 + miR-195-5p inhibitor NC} and HCT116^{Lv-anti-SNHG16 + miR-195-5p inhibitor} were shown as bar graphs. **B:** The protein quantitation of YAP1 expression from DLD1^{Blank}, DLD1^{Lv-Oe-SNHG16-NC}, DLD1^{Lv-Oe-SNHG16 + miR-195-5p mimics NC}, and DLD1^{Lv-Oe-SNHG16 + miR-195-5p mimics} were shown as bar graphs. Statistical analysis was conducted using one-way ANOVA. Error bars, SEM. ***p* < 0.01.

supplementary figures

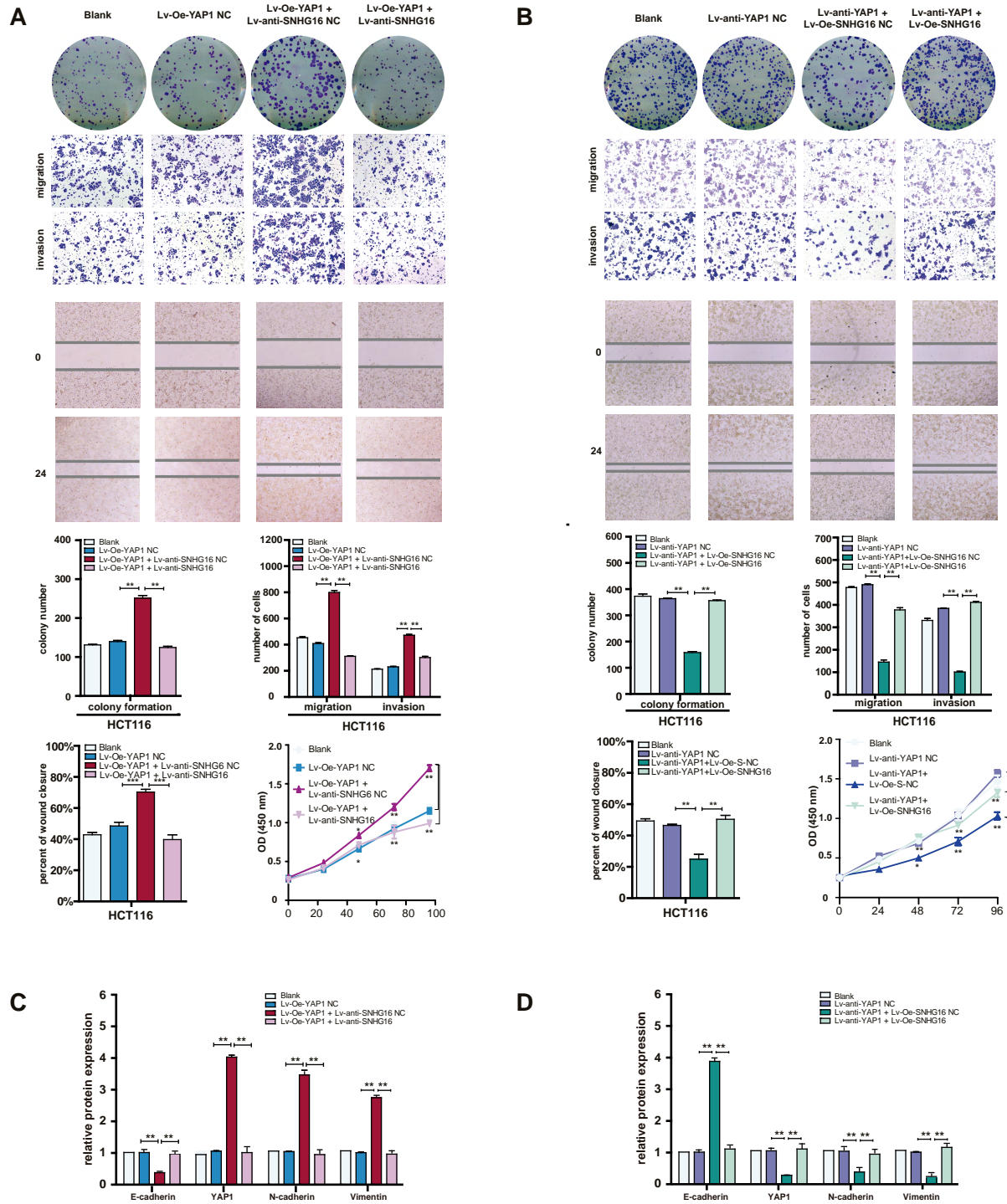
Supplementary Fig 5. The effect of YAP1 on tumor colony formation, migration, invasion, and EMT of CRC



A-B: Colony formation assay was performed in CRC cell lines following YAP1 knockdown or overexpression. **C-D:** Graphical representation of transwell showing migration and invasion ability of HCT116 after YAP1 knockdown (C) or overexpression (D). **E-F:** Wound healing assay was performed in CRC cell lines following YAP1 knockdown (E) or overexpression (F). **G-H:** The quantitation of EMT markers expression from YAP1 knockdown (G) or overexpression (H) CRC cell lines was shown as bar graphs. All representative data are from three independent experiments. Statistical analysis was conducted using one-way ANOVA. Error bars, SEM. ** $p < 0.01$.

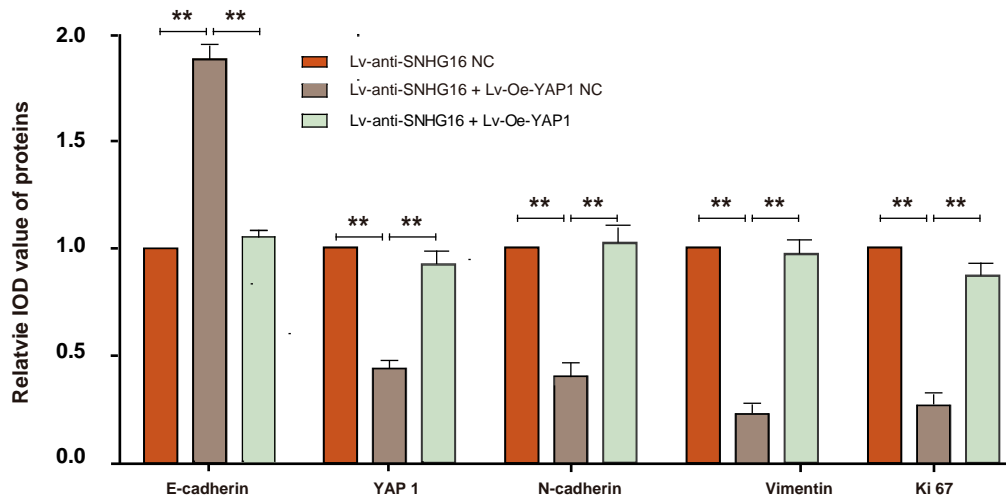
supplementary figures

Supplementary Fig 6. The effect of YAP1-SNHG16 positive feedback loop on the progression of tumor.



A: The colony formation, migration, invasion and proliferation in HCT116^{Blank}, HCT116^{Lv-Oe-YAP1-NC}, HCT116^{Lv-Oe-YAP1 + Lv-anti-SNHG16-NC}, and HCT116^{Lv-Oe-YAP1 + Lv-anti-SNHG16} were detected by colony formation, wound healing, transwell assay, and cck8. **B:** Colony formation, cck8, wound healing, and transwell assay were performed in HCT116^{Blank}, HCT116^{Lv-anti-YAP1-NC}, HCT116^{Lv-anti-YAP1 + Lv-Oe-SNHG16-NC}, and HCT116^{Lv-anti-YAP1 + Lv-Oe-SNHG16}. **C:** The quantitation of protein expression from HCT116^{Blank}, HCT116^{Lv-Oe-YAP1-NC}, HCT116^{Lv-Oe-YAP1 + Lv-anti-SNHG16-NC}, and HCT116^{Lv-Oe-YAP1 + Lv-anti-SNHG16} were shown as bar graphs. **D:** The quantitation of protein expression from HCT116^{Blank}, HCT116^{Lv-anti-YAP1-NC}, HCT116^{Lv-anti-YAP1 + Lv-Oe-SNHG16-NC}, and HCT116^{Lv-anti-YAP1 + Lv-Oe-SNHG16} were shown as bar graphs. All representative data are from three independent experiments. Statistical analysis was conducted using one-way ANOVA. Error bars, SEM. ** $p < 0.01$.

supplementary figures



Supplementary Fig 7: Comparison of relative integrated optical density (IOD) values of Ki67 and EMT related markers among HCT116^{Lv-anti-SNHG16-NC}, HCT116^{Lv-anti-SNHG16 + Lv-Oe-YAP1 NC}, HCT116^{Lv-anti-SNHG16 + Lv-Oe-YAP1}. All representative data are from three independent experiments. Statistical analysis was conducted using one-way ANOVA. Error bars, SEM. **p < 0.01.

151 **REFERENCE**

152 1 Sun M, Song HB, Wang SY, et al. Integrated analysis identifies microRNA-195 as a suppressor
153 of Hippo-YAP pathway in colorectal cancer. *Journal of hematology & oncology*. 2017; 10.

154 2 Martinotti S, Ranzato E. Scratch Wound Healing Assay. *Methods in molecular biology (Clifton,*
155 *NJ)*. 2020; 2109: 225-229.

156